Dalton Transactions

Cite this: *Dalton Trans.*, 2011, **40**, 1338

www.rsc.org/dalton

PAPER

Copper(II) complexes of hybrid hydroxyquinoline-thiosemicarbazone ligands: GSK3β inhibition due to intracellular delivery of copper†

James L. Hickey,[a] Peter J. Crouch,[b,c] Sithorn Mey,[a] Aphrodite Caragounis,[b] Jonathan M White,[a] Anthony R. White[b,c] and Paul S. Donnelly*[a]

Received 6th September 2010, Accepted 25th November 2010
DOI: 10.1039/c0dt01176b

Cognitive decline associated with Alzheimer's disease appears to be related to the hyper-phosphorylation of the protein tau as a consequence of increased activity of glycogen synthase kinase 3β (GSK3β), and subsequent formation of neurotoxic neurofibrillary tangles. Abberant metal ion homeostasis, particularly involving copper has been implicitly linked to the pathogenesis of the disease. Increasing intracellular copper concentrations has been found to trigger pathways that result in inhibition of GSK3β. The syntheses and characterisation of tetradentate hybrid hydroxyquinoline-thiosemicarbazone proligands is presented. The ligands form stable complexes with Cu^{II} where the copper ion is four coordinate and essentially square planar as characterised by single crystal X-ray crystallography. The reduction of the metal ion to Cu^{I} has been studied by electrochemical techniques and occurs at potentials that permit intracellular reduction. The new complexes show class dependent cell membrane permeability in neuronal-like SH-SY5Y cells with subsequent increases in intracellular copper concentrations. The increased intracellular copper results in a dose-dependent inhibition (phosphorylation) of GSK3β.

Introduction

Alzheimer's disease (AD) is a progressive neurodegenerative disease that leads to synaptic failure and neuronal death. These symptoms can initially manifest as mild forgetfulness but progress to complete loss of cognition and ultimately death.[1] Characteristic pathological hallmarks of the disease include the presence of extracellular senile plaques and intracellular neurofibrillary tangles in the brain. The plaques are comprised of insoluble aggregated peptide amyloid-β (Aβ), a 39–43 amino acid peptide derived from the amyloid precursor protein (APP).[2–4] These amyloid plaques do not consistently correlate with cognitive impairment and some argue that smaller soluble oligomeric species are the toxic species responsible for neuronal death.[1]

Neurofibrillary tangles (NFT) consist of a hyper-phosphorylated form of a microtubule-associated protein called tau. NFT initiate with the formation of bundles of paired helical filaments that accumulate in the neuronal cytoplasm. The hyper-phosphorylation of tau results in its detachment from microtubules that consequently lose structural integrity with concomitant impaired axonal transport and compromised synaptic function.[5] Importantly, NFT burden does correlate with the severity of cognitive impairment and some evidence supports a key downstream role for tau hyper-phosphorylation in Aβ-mediated neuronal degeneration.[6]

Recent developments have highlighted the importance of metal ion homeostasis in the development of Alzheimer's disease and potential therapeutic strategies have focused on targeting copper metabolism.[7–11] Both Aβ and APP are known to bind to copper and there is evidence that brain Cu metabolism is altered in AD. APP-knockout mice have elevated levels of Cu in the cerebral cortex, whilst APP-over-expressing mice have reduced brain Cu levels.[12–15] Promising results have been obtained with 8-hydroxyquinoline derivatives such as clioquinol **1** (Fig. 1a) that are known to bind Cu^{II} and other metal ions as well as hydroxypyridone derivatives.[16–18] The mode of action of these ligands was thought to involve chelation of metals bound to Aβ, resulting in dissolution of amyloid aggregates. However, it is now thought that the hydroxyquinoline derivatives may also act as ionophores by chelating extracellular Cu to form membrane permeable copper complexes that activate neuroprotective cell signalling pathways by increasing cellular metal ion bioavailability.[19] Central to this neuroprotective cell signalling pathway is the inhibition of glycogen synthase kinase 3β (GSK3β), a serine and threonine protein kinase responsible for certain intracellular phosphorylation reactions. GSK3β is a constitutively active kinase and is inactivated by phosphorylation at the serine-9 residue. Importantly, increased GSK3β activity

[a]*School of Chemistry and Bio21 Molecular Science and Biotechnology Institute, University of Melbourne, Parkville, Melbourne, Victoria, 3010, Australia. E-mail: pauld@unimelb.edu.au*
[b]*Centre for Neuroscience and Department of Pathology, University of Melbourne, Parkville, Melbourne, Victoria, 3010, Australia*
[c]*Mental Health Research Institute of Victoria, Parkville, Melbourne, Victoria, 3052, Australia*

† CCDC reference numbers 801975–801977. For crystallographic data in CIF or other electronic format see DOI: 10.1039/c0dt01176b

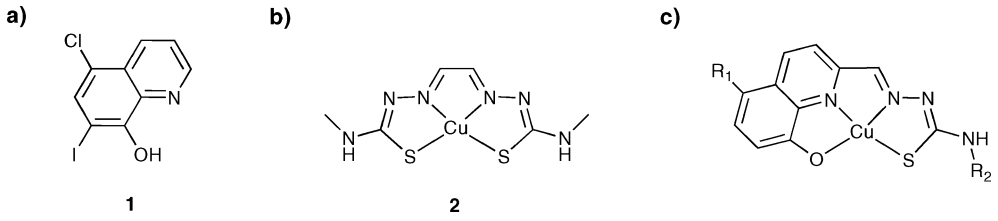

1 2

Fig. 1 **a)** Cu^{II} chelating 8-hydroxyquinoline clioquinol **1**, **b)** *bis*(thiosemicarbazonato) Cu^{II} complex, Cu^{II}(gtsm) **2**, and **c)** hybrid hydroxyquinoline-thiosemicarbazone Cu^{II} complexes.

(through decreased phosphorylation at serine-9) has been linked to tau hyperphosphorylation and NFT formation, and increased GSK3β activity is induced by exposure to Aβ.[20] Abnormal GSK3β activity may also be central to a number of other brain disorders, and as a consequence inhibition of GSK3β is seen an important target.[21,22]

We recently reported an alternative therapeutic approach using a stable cell permeable *bis*(thiosemicarbazonato) Cu^{II} complex, Cu^{II}(gtsm) **2** (Fig. 1b) for the controlled intracellular delivery of Cu that resulted in improved cognition in an animal model of AD. Cu^{II}(gtsm) is a neutral low molecular weight complex that is membrane permeable. The Cu^{II} complex is very stable (K_a = 10^{18} M) but once the complex enters the reducing environment encountered in most cells the Cu^{II} is susceptible to reduction to Cu^{I}. The ligand has a lower affinity for Cu^{I} ($K_a \sim 10^{10-13}$ M) so the copper becomes essentially bio-available with transfer of Cu^{I} to copper chaperone proteins with higher affinity for Cu^{I}.[23] We were able to show that Cu^{II}(gtsm) inhibited GSK3β and decreased tau phosphorylation in cell culture and animal models of AD.[24,25]

Stimulated by the success of both hydroxyquinoline and thiosemicarbazone Cu^{II} complexes in inhibiting GSK3β respectively, we have combined both types to prepare two new classes of tetradentate hybrid hydroxyquinoline-thiosemicarbazone proligands and their Cu^{II} complexes (Fig. 1c). The new complexes show class dependent membrane permeability in a cultured neuronal-like cell line and subsequent potent phosphorylation (inhibition) of GSK3β.

Results and discussion

Synthesis and characterisation of hybrid hydroxyquinoline-thiosemicarbazone Cu^{II} complexes

Tetradentate hybrid hydrazinopyridine-thiosemicarbazones have been investigated previously as proligands for potential hypoxia selective Cu^{II} radiopharmaceuticals and two hybrid hydroxyquinoline-thiosemicarbazonato copper(II) complexes have been evaluated for their anti-cancer activity in a neuroblastoma cell line.[26,27] This is the first report outlining the synthesis of six new hybrid hydroxyquinoline-thiosemicarbazone proligands and their copper complexes along with their ability to deliver copper into cells and the subsequent effects on the activity of GSK3β.

The new proligands **3**, **4** and **5** were prepared in good yields by condensation reactions catalysed by acetic acid between 2-formyl-8-hydroxyquinoline and a 4-*N*-substituted-3-thiosemicarbazide in ethanol. All were characterised by ^{1}H nmr, ^{13}C nmr, ESI mass spectrometry and microanalysis; with the purity of each ligand confirmed by reverse phase high pressure liquid chromatography (RP-HPLC) (Scheme 1).

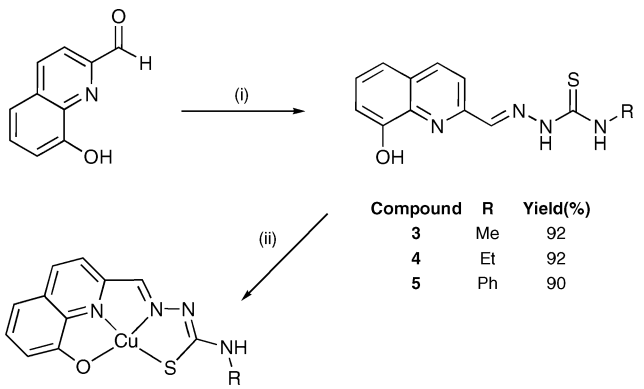

Compound	R	Yield(%)
3	Me	92
4	Et	92
5	Ph	90

Compound	R	Yield(%)
6	Me	92
7	Et	89
8	Ph	96

Scheme 1 *Reagents and conditions*: (i) 4-*N*-substituted-3-thiosemicarbazide, cat. AcOH, EtOH, rf for 4 h; (ii) $Cu(OAc)_2 \cdot 2H_2O$, DMF, rt for 4 h.

A crystal of **3** suitable for X-ray crystallography was grown by evaporation of a methanol solution of the ligand (Fig. 2). The proligand has crystallised in the *E* isomeric form with the thiosemicarbazone functional group extending away from the aromatic ring and the molecule is essentially planar. The C11–S1 bond distance, 1.689(2) Å, and C10–N3 distance, 1.282(2) Å suggests the "free" ligand is best represented in the tautomeric form shown in Scheme 1. A ^{1}H nmr spectrum of **3** in d_6-dmso reveals a single isomer with evidence of H-coupling for the N*H*–CH_3 and the substituent methyl. The quaternary *C*=S results in a signal at δ 178 ppm in the ^{13}C nmr spectrum whereas the N=*C*H results in a resonance at δ 141.8 ppm.

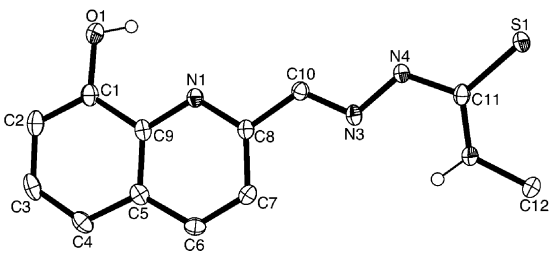

Fig. 2 An ORTEP (40% probability) representation of molecular structure of **3**. Select hydrogen atoms have been omitted for clarity.

The nmr spectra of **4** and **5** are similar to **3** where appropriate, and again suggest a single isomer dominates in d_6-dmso solution. RP-HPLC confirmed the purity of the ligands (C_{18} column (4.6 × 150 mm, 5 mm) with a 1 mL min^{-1} flow rate and UV spectroscopic detection at 214 nm, 220 nm, and 270 nm. Retention times (R_t/min) were recorded using a water–acetonitrile gradient elution method). With the retention times suggesting a systematic increase in lipophilicity (**3**, R_t = 9.48 min; **4**, R_t = 10.71 min; and **5**, R_t = 13.27 min).

The Cu^{II} complexes **6**, **7**, and **8** can be prepared by addition of $Cu^{II}(OAc)_2 \cdot 2H_2O$ to a solution of proligand in dimethyl formamide at ambient temperature (Scheme 1). The immediate colour change to deep red indicates complexation is very rapid and the neutral Cu^{II} complexes can be readily precipitated by the addition of water. In each case the ESI mass spectrum reveals a peak at the expected *m*/*z* value corresponding to $[Cu^{II}\mathbf{L} + H^+]$ with the expected isotope pattern.

A representation of the molecular structure of the neutral Cu^{II} complex **6** as determined by single crystal X-ray crystallography is shown in Fig. 3. The Cu^{II} is 4-coordinate with the dianionic tetradentate ligand coordinating through a deprotonated phenolic oxygen, nitrogen of the substituted quinoline ring, the azamethinic nitrogen and thiolate sulfur. The coordination geometry about the copper is distorted square planar with a 5-5-5 (*O*,*N*,*N*,*S*) chelate ring system. The N2–Cu–S1 bond angle (85.7(1)°) is significantly larger than the N1–Cu–O1 bond angle of 81.9(1)°. The Cu–S bond distance (2.223(1) Å) and Cu–N azamethinic distance (1.999(4) Å) are similar to the analogous distance in Cu^{II}(gtsm).[28] Deprotonation to give the thiosemicarbazonato limb of the ligand is reflected in the C11–S1 distance of 1.767(5) Å, suggesting more thiolate-like character than the thione-like 'free' ligand **3** (C11–S1 = 1.689(2) Å) along with a marginally shorter N3–C11 bond distance of 1.334(6) Å than N4–C11 in $H_2\mathbf{L}^1$ (1.363(2) Å), suggesting more double bond-like character. Crystals of **8** were grown by evaporation of a saturated solution of the complex in ethanol. A representation of the molecular structure (Fig. 4) reveals the copper binding to the ligand *via* the hydrazinic nitrogen, rather than azamethinic nitrogen, creating a 4-membered N–Cu–S chelate ring. This binding mode in thiosemicarbazonato metal complexes is rare but precedents include *bis*(thiosemicarnazonato)nickel(II) complexes,[29,30] a single *bis*(thiosemicarnazonato)zinc(II) complex and thiosemicarbazonato(ruthenium(II)) complexes.[31]

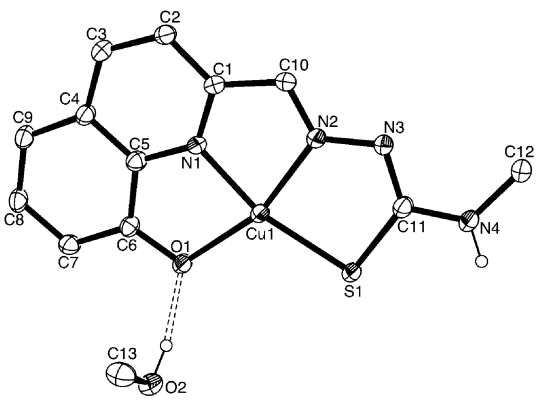

Fig. 3 An ORTEP representation (40% probability) of **6**·CH_3OH. Select hydrogen atoms have been omitted for clarity.

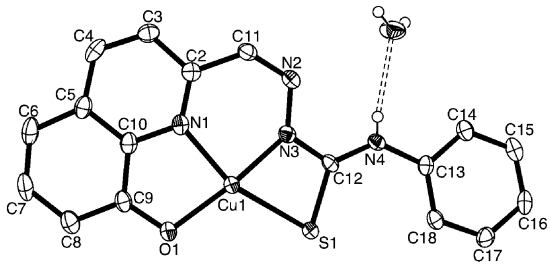

Fig. 4 An ORTEP representation (40% probability) of **8**·H_2O. Select hydrogen atoms have been omitted for clarity.

The Cu^{II} is essentially 4-coordinate with weak axial interactions with a sulfur atom of an adjacent molecule Cu–S′ = 2.975(1) Å and short π–π contacts (*ca*. 3.5 Å) to give infinite chains (Fig. 5). The relatively unusual coordination mode results in a N1–Cu–N3 bond angle of 89.(1)° and a N3–Cu–S1 bond angle of 70.2(1)°. The synthesis of the copper complexes of 8-hydroxyquinoline-2-carboxaldehyde-3-thiosemicarbazone and 8-hydroxyquinoline-2-carboxaldehyde-*N*-4,4′-dimethyl-3-thiosemicarbazone have been reported recently but this is the first report of the copper complexes of the *N*-4-methyl, *N*-4-ethyl and *N*-4-phenyl derivatives and the first structural characterization by X-ray crystallography of copper complexes of this family of tetradentate ligand.

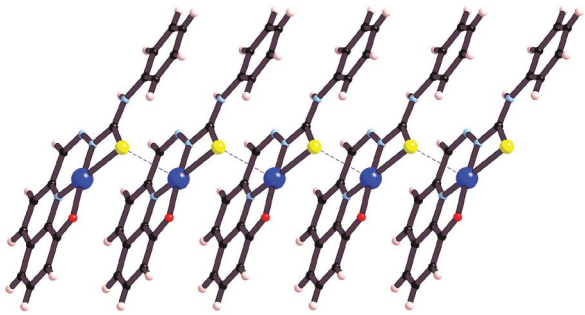

Fig. 5 A representation of the polymeric molecular array of **8** displaying short contacts between Cu–S′ = 2.975(1) Å.

The complexes **6–8** have limited solubility in water, so it was of interest to prepare water-soluble derivatives. The introduction of a sulfonic acid to the backbone of the hydroxyquinoline *para* to the phenolic hydroxyl position improved the solubility of both the ligand and complex in aqueous environments without interfering with complexation of Cu^{II}. An initial attempt to oxidise 2-methyl-8-hydroxyquinoline-5-sulfonic acid to an aldehyde with SeO_2 failed due to the insolubility of the acid in respective ethereal solvents. The selective oxidation does proceed cleanly from the 2-methyl-8-hydroxyquinoline-5-sulfonyl chloride **9** to the aldehyde **10**. Subsequent hydrolysis of the sulfonyl chloride in an acetone/water mixture (50/50) gave the desired 2-formyl-8-hydroxyquinoline-5-sulfonic acid **11** in good yield (78%) (Scheme 2).

The sulfonated proligands **12**, **13** and **14** were prepared in an analogous manner to **3–5**, *via* standard condensation reactions between 2-formyl-8-hydroxyquinoline-5-sulfonic acid and a 4-*N*-substituted-3-thiosemicarbazide in ethanol at ambient temperature (Scheme 3). An additional acid catalyst was not necessary as the reactions were found to proceed rapidly and in sufficient yields. The new sulfonated derivatives were characterised by ^1H nmr, ^{13}C

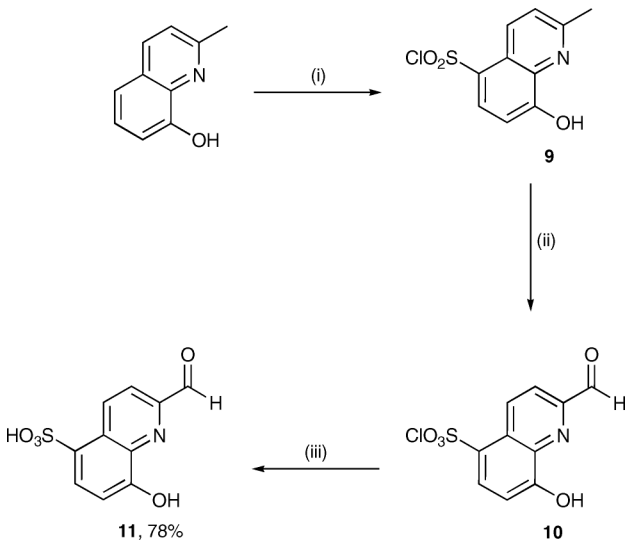

Scheme 2 *Reagents and conditions*: (i) Chlorosulfonic acid, neat, rt 1 h; (ii) SeO_2, Dioxane, rf 12 h; (iii) H_2O, Acetone/H_2O, rt 1 h.

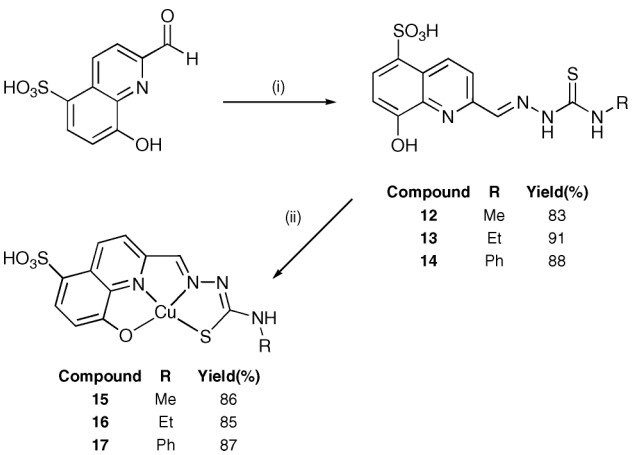

Compound	R	Yield(%)
12	Me	83
13	Et	91
14	Ph	88

Compound	R	Yield(%)
15	Me	86
16	Et	85
17	Ph	87

Scheme 3 *Reagents and conditions*: (i) 4-*N*-substituted-3-thiosemicarbazide, EtOH, rt for 4 h; (ii) $Cu(OAc)_2{\cdot}2H_2O$, DMF, rt for 4 h.

nmr, ESI mass spectrometry and microanalysis; with the purity of each ligand confirmed by RP-HPLC. The retention times are significantly lower than observed for **3–5** as a result of the polar sulfonic acid, but also suggest a systematic increase in lipophilicity (**12**, R_t = 6.86 min, **13**, R_t = 7.69 min and **14**, R_t = 9.67 min).

The ^{1}H nmr spectra of proligands **12–14** in d_6-dmso are similar to that of **3–5** in that a single isomer dominates in solution and H-coupling is observed for the N*H*-R to a neighbouring alkyl substituent. The inductive effect of the sulfonic acid results in a general (and in some cases significant) shift of ~ 1 ppm downfield in the hydroxyquinoline aromatic signals. The phenolic signal observed in **3–5** (~9.83 ppm) is not resolved, instead exchanging with the sulfonic acid and adventitious water. The absence of resonances attributed to the quaternary *C*–OH and *C*–SO_3H in the ^{13}C nmr spectra of **12–14** also suggests rapid exchange on the nmr timescale. A signal at δ ~178 ppm in the ^{13}C nmr spectra of **12–14** attributed to *C*=S is similar to that observed for **3–5**, whereas a resonance observed at δ ~150 ppm assigned as the N=*C*H is somewhat downfield (~10 ppm) of the analogous signal in the spectra of **3–5**.

The Cu^{II} complexes of the sulfonated proligands were also prepared by addition of $Cu^{II}(CH_3CO_2)_2{\cdot}H_2O$ to a solution of **12–14** in dimethyl formamide at ambient temperature (Scheme 3). An immediate colour change to deep red was observed indicating rapid complexation. The crude neutral Cu^{II} complexes **15–17** were precipitated by the addition of diethyl ether and collected. On redissolving in water the complexes were readily purified on a cation-exchange column. Characterisation for each complex was confirmed by microanalysis and an ESI mass spectrum that revealed a peak at the expected *m/z* value corresponding to [Cu^{II}**L** + H^+] with the expected isotope pattern.

Monitoring the stability of Cu^{II} complex 6 with biological molecules by UV/Vis absorbance

The proligand **3** displays characteristic absorbances in the electronic spectrum at λ_{abs} = 315 nm (ε = 8.4 × 10^4 M^{-1}) and 350 nm (ε = 9.85 × 10^4 M^{-1}) that are also present in the spectra of **4** and **5**. Complexation with Cu^{II} to give **6** results in two distinct red shifted chromophoric absorbances at λ_{abs} = 326 nm (ε = 5.36 × 10^4 M^{-1}) and 402 nm (ε = 2.71 × 10^4 M^{-1}) as well as a broad absorbance centred at λ_{abs} = 490 nm (ε = 6.5 × 10^3 M^{-1}) characteristic of ligand to metal charge transfer transition. Complexes **7** and **8** display similar spectra. The characteristic absorbance at λ_{abs} = 402 nm was chosen to monitor the stability of Cu^{II} complex **6** in the presence of competing biologically relevant ligands L-histidine and L-cysteine and the biological reducing agent ascorbic acid. A solution of **6** in an aqueous buffer (pH 7.4) was incubated in the presence of a 10-fold excess of L-histidine, L-cysteine and ascorbic acid (30% DMSO/PB, 1 mM, pH 7.4) over 24-hours at 37 °C. During this period minimal change in the absorbance spectra of Cu^{II} complex **6** were detected showing it is likely that the complexes have sufficient stability in extracellular media to serve as chaperones for intracellular delivery of Cu.

Electrochemistry

Measurements of reduction potentials in dimethylformamide (DMF) or dimethylsulfoxide (DMSO) have proved useful in predicting the retention of copper inside the cell, with clear correlations between the reduction potential and likely intracellular reduction.[32] The Cu^{II} complex of the *bis*(thiosemicarbazone) proligand derived from diacetyl, Cu^{II}(atsm) = (diacetyl-bis(4-*N*-methyl-3-thiosemicarbazonato)copper(II), selectively accumulates in hypoxic cells and is being investigated as a hypoxia tracer for positron emission tomography. In comparison, the ligand derived from glyoxal, Cu^{II}(gtsm) **2** (Fig. 1) is easier to reduce than Cu^{II}(atsm) by some 160 mV (Cu^{II}(gtsm) E_m = –0.44 V compared with Cu^{II}(atsm) E_m = –0.60 V *vs.* SCE).[23,33] As a result, the reducing environment encountered inside most cells is sufficient to reduce the metal ion in Cu^{II}(gtsm) to Cu^{I}. The ligand has a lower affinity for Cu^{I} (K_D ~ 10^{-13} M) so the copper becomes essentially bioavailable with transfer of Cu^{I} to copper chaperone proteins with higher affinity for Cu^{I}.[23] In comparison, Cu^{II}(atsm) is harder to reduce and unless cells are hypoxic the complex remains intact with the metal ion remaining bound to the ligand.

The electrochemical properties of the complexes **6–8** were investigated by cyclic voltammetry. The complexes all undergo an essentially irreversible reduction at E_{pc} = –0.49 V (*vs.* SCE) at

a glassy carbon electrode which can be attributed to a Cu^{II}/Cu^{I} process. The initial reduction is followed by two related oxidative events at E_{pa} = –0.36 V and 0.05 V. This suggests that the initial electrochemical change is followed by a chemical change. The irreversible reduction, Cu^{II}/Cu^{I} process of **6–8** (E_{pc} = –0.49 V) is close to that of Cu^{II}(gtsm) **2** (E_{pc} = –0.48 V),[23] suggesting that the reducing environment encountered in most cells may be sufficient to reduce the metal ion to Cu^{I} that will dissociate from the hydroxyquinoline-thiosemicarbazone ligand in the presence of competing ligands found inside cells.

Cell biology

Neuronal-like SH-SY5Y cells were treated with the Cu^{II} compounds **6–8** and **15–17** at 0, 1, 5 or 10 μM for 1 h; cellular levels of Cu were then measured by inductively coupled plasma mass spectrometry (ICP-MS). Data presented in Fig. 6 indicates that Cu^{II} compounds **6–8** are all cell permeable and increase cellular Cu levels in a dose-dependent manner. By contrast, the sulfonated variants **15–17** did not increase cellular levels of Cu indicating these compounds were not cell permeable. As **6–8** all showed a comparable dose-dependent uptake effect, **6** was chosen to represent the membrane permeable compounds. Whereas **15** was also tested as a representative of the complexes that did not increase intracellular copper.

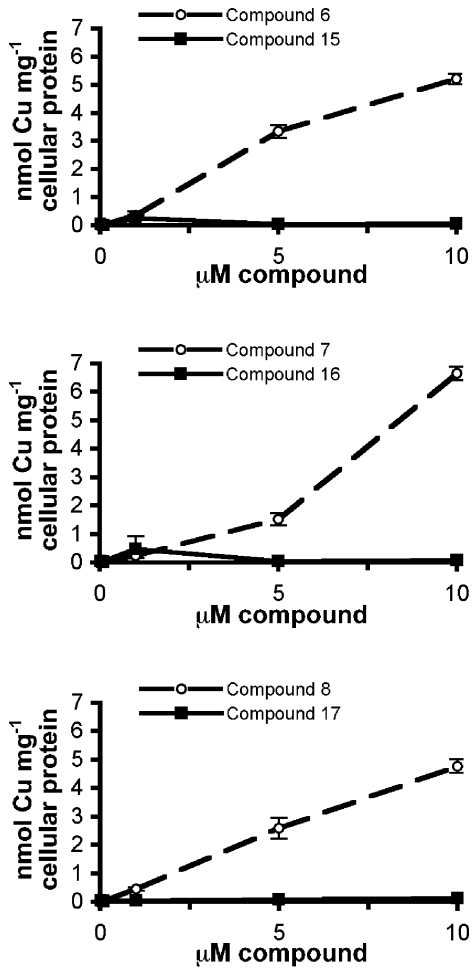

Fig. 6 Cu content of cell samples after treating with Cu^{II} complexes **6–8** and sulfonated Cu^{II} complexes **15–17** at the concentrations shown for 1 h. Metal ion content is expressed relative to cellular protein.

The effects of complexes **6** and **15** on cell viability was investigated using two different methods (Fig. 7). The dose-dependent increase in cellular Cu induced by treatment with **6**, correlated with a decrease in cellular capacity to reduce MTS (5-(3-carboxymethoxyphenyl)-3-(4,5-dimethylthiazol-2-yl)-2-(4-sulfophenyl)-2*H*-tetrazolium), indicating decreased activity of cellular reductases. The water soluble sulfonated analogue, compound **15**, had no effect on the cells ability to reduce MTS, consistent with the cell-uptake data that shows that the water soluble compound is not membrane permeable. This diminished ability to reduce MTS does not necessarily imply a loss of cell viability and correlations between the MTS assays and cytotoxicity are to be treated with caution.

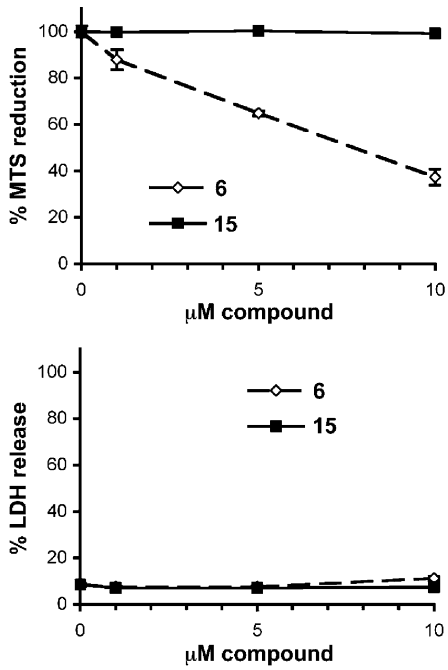

Fig. 7 Relative effects of **6** and **15** on the activity of cellular reductases (MTS reduction) and LDH release. MTS data are expressed relative to values obtained for cells treated with 0 μM compound. LDH data are expressed relative to cells treated with 0.1% (v/v) Triton-X 100 to induce plasma membrane permeabilisation and complete LDH release.

An alternative plasma membrane permeabilisation assay measures lactate dehydrogenase (LDH) release. In this assay compound **6** had no effect on LDH release, indicating the compound did not induce membrane permeabilisation and cell death (Fig. 7). The MTS reduction results are consistent with previous work describing that cell viability assays based on endocytosis/exocytosis mechanisms, such as the MTS assay, can be misleading given the capacity for Cu-based metal–ligand complexes to alter endocytosis/exocytosis.[34]

An analysis of cell lysates following treatment with **6** or **15** revealed that the increase in cellular Cu mediated by **6**, correlated with increasing inhibitory phosphorylation of GSK3β (Fig. 8). This result is consistent with previous *in vitro* and *in vivo* work using metal–ligand complexes capable of increasing bio-available

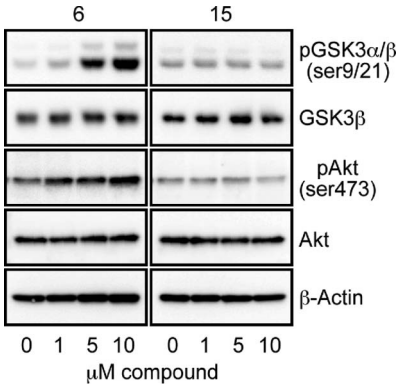

Fig. 8 Relative effects of **6** and **15** on levels of total and phosphorylated forms of GSK3β and Akt. Complex **6** but not **15** induces inhibitory phosphorylation of GSK3β (serine-9 residue) and activating phosphorylation of Akt (serine-473) in a dose-responsive manner.

intracellular Cu.[19,24,25,35,36] In comparison, treatment with the water soluble analogue **15** had no effect on levels of GSK3β consistent with the lack of uptake indicated by ICP-MS.

To partly examine the cellular mechanisms leading to the inhibitory phosphorylation of GSK3β by **6**, we also examined effects of the compound on phosphorylation of the signalling kinase Akt (Fig. 8). The kinase activity of Akt is activated once it is phosphorylated at serine-473, and like GSK3β, Akt phosphorylation in SH-SY5Y cells increased with increasing concentration of **6** (Fig. 8). These data indicate the phosphorylation of GSK3β mediated by **6** may be a downstream consequence of Akt activation since Akt is widely recognised for its capacity to phosphorylate GSK3β at serine-9.[37]

Concluding remarks

A series of new tetradentate hybrid hydroxyquinoline-thiosemicarbazone proligands were prepared that doubly deprotonate to form neutral Cu^{II} complexes. Water-soluble analogues were prepared by the introduction of a sulfonate functional group in the 5-position of the hydroxyquinoline. The Cu^{II} complexes were characterised by microanalysis, ESI-MS and electronic spectroscopy. The molecular structure of two of the Cu^{II} complexes were determined by single crystal X-ray crystallography confirming for the first time a 4-coordinate distorted square planar (*O*,*N*,*N*,*S*) coordination environment for the copper(II) atom, whilst revealing an unusual coordination motif of a 4-membered N–Cu–S chelate ring for complex **8**. The copper(II) complexes were stable in aqueous buffer solutions to a histidine/cysteine challenge suggesting that formed complexes are of sufficient stability for biological applications. Electrochemical measurements using cyclic voltammetry revealed that the complexes were susceptible to an irreversible reduction attributed to a Cu^{II}/Cu^{I} reduction at potentials that could be encountered in the reducing environment found inside most cells. In the case of the membrane permeable copper complexes the accumulation of Cu elicited a dose-dependent inhibitory phosphorylation of both GSK3β and signalling kinase Akt. The introduction of a sulfonate functional group allowed the formation of water soluble analogues but these derivatives were not membrane permeable in the cell lines tested and did not elicit an increase in intracellular copper concentrations and consequently did not phosphorylate GSK3β or signalling kinase Akt. Cells operate at an overall reducing environment and there have been some attempts to quantify the redox environment of cells.[38] It is proposed that once the complex is inside the cell the metal ion is reduced and released from the hydroxyquinoline-thiosemicarbazone ligand in the presence of competing Cu^{I} ligands found in cells. An alternative explanation of the observed behaviour is that the complexes are reduced and the metal ion dissociated from the ligand at the cell surface or witihin the cell membrane followed by uptake of Cu^{I} into the cell. Both possibilites would lead to an increase in bioavailable Cu^{I} inside the cell that results in inhibitory phosphorylation of GSK3β.[34] The hybrid ligands present a controlled way of delivering copper ions intracellularly. This results in inactivation of GSK3β, a major kinase involved in the hyper-phosphorylation of tau an event that appears central to the pathological progression of Alzheimer's disease. We have shown that increased intracellular Cu has a profound effect on the activity of GSK3β. This finding is significant, considering the recent success of therapeutic approaches that modulate Cu metabolism.

Table 1 Crystallographic data

	3	**6**	**8**
Chemical formula	$C_{12}H_{12}N_4OS$	$[C_{12}H_{10}N_4OSCu]\cdot[CH_3OH]$	$[C_{17}H_{12}CuN_4OS]\cdot[H_2O]$
M	260.32	353.88	401.92
Crystal system	Monoclinic	Triclinic	Orthorhombic
T/K	130.0(2)	130.0(2)	130.0(2)
Space group	$P2_1/c$	$P\bar{1}$	$P2_12_12_1$
a/Å	10.394(1)	7.9196(7)	4.0657(2)
b/Å	7.0021(8)	9.5097(10)	14.7702(8)
c/Å	16.770(2)	10.0744(11)	26.266(1)
α (°)	90	91.711(9)	90
β (°)	98.544(2)	90.001(8)	90
γ (°)	90	111.220(9)	90
V/Å^3	1207.0(2)	706.93(12)	1577.3(1)
Z	4	2	4
Independent refl.	2118	2735	2707
R_{int}	0.029	0.033	0.046
$R(I > 2\sigma(I))$	0.0388	0.0387	0.0452
wR(all data)	0.0984	0.1599	0.1067

Experimental

Crystallography

Crystals of **3**, **6**, and **8**, respectively were mounted in low temperature oil then flash cooled to 130 K using an Oxford low temperature device. Intensity data were collected at 130 K with an Oxford XCalibur X-ray diffractometer with Sapphire CCD detector using Cu-Kα radiation (graphite crystal monochromator λ = 1.54184 Å) (Table 1). Data were reduced and corrected for absorption.[39] The structures were solved by direct methods and difference Fourier synthesis using the SHELX suite of programs[40] as implemented within the WINGX[41] software. Thermal ellipsoid plots were generated using the program ORTEP-3[42] integrated within the WINGX suite of programs.

General procedures

Syntheses. All reagents and solvents were obtained from commercial sources (Sigma–Aldrich) and used as received unless otherwise stated. 2-Formyl-8-hydroxyquinoline[43] and 2-methyl-8-hydroxyquinoline-5-sulfonyl chloride (**9**)[44] were prepared according to previously reported procedures. Cation-exchange chromatography was performed on DOWEX® 50WX2-200 ion-exchange resin (H^+ form 1.5 cm × 10 cm). Elemental analyses for C, H, and N were carried out by Chemical & MicroAnalytical Services Pty. Ltd, Vic. NMR spectra were recorded on a Varian FT-NMR 500 spectrometer (^{1}H NMR at 499.9 MHz and ^{13}C{^{1}H} NMR at 125.7 MHz) at 298 K and referenced to the internal solvent residue.[45] Mass spectra were recorded on an Agilent 6510-Q-TOF LC/MS mass spectrometer and calibrated to internal references.

UV/Visible spectroscopy. UV/Vis spectra were recorded on a Cary 300 Bio UV-Vis spectrophotometer, from 800–200 nm at 0.5 nm data intervals with a 600 nm min^{-1} scan rate. Solutions of complex **6** in 30% DMSO/PB (1 mM, pH 7.4) was incubated in the presence of a 10-fold excess of L-histidine, ascorbic acid and L-cysteine and monitored over 24-hours at 37 °C.

High pressure liquid chromatography. Analytical RP-HPLC traces were acquired using an Agilent 1200 series HPLC system equipped with a Agilent Zorbax Eclipse XDB-C18 column (4.6 × 150 mm, 5 mm) with a 1 ml min^{-1} flow rate and UV spectroscopic detection at 214 nm, 220 nm, and 270 nm. Retention times (R_t/min) were recorded using a gradient elution method of 0–100% B over 25 min, solution A consisted of water (buffered with 0.1% trifluoroacetic acid) and solution B consisted of acetonitrile (buffered with 0.1% trifluoroacetic acid).

Electrochemistry. Cyclic voltammograms were recorded using an AUTOLAB PGSTAT100 equipped with GPES V4.9 software. Measurements of the complexes were carried out at approximately 1 × 10^{-4} M in dimethylformamide with tetrabutylammonium tetrafluoroborate (1 × 10^{-2} M) as electrolyte using a glassy carbon disk (d, 3 mm) working electrode, a Pt wire counter/auxiliary electrode, and a Ag/Ag$^+$ pseudo reference electrode (silver wire in CH_3CN (Bu_4NBF_4) (0.1 M) $AgNO_3$ (0.01 M)). Ferrocene was used as an internal reference (E_m(Fc/Fc$^+$) = 0.54 V *vs.* SCE), where E_m refers to the midpoint between a reversible reductive (E_{pc}) and oxidative (E_{pa}) couple, given by $E_m = (E_{pc}+E_{pa})/2$. Irreversible systems are only given reductive (E_{pc}) and oxidative (E_{pa}) values, respectively.

Synthetic procedures

2-Formyl-8-hydroxyquinoline-5-sulfonic acid (11). 2-Methyl-8-hydroxyquinoline-5-sulfonyl chloride (836 mg, 3.24 mmol) was dissolved in dry dioxane (40 mL) and refluxed with SeO_2 (400 mg, 3.57 mmol) for 12 h. On cooling, the selenium precipitate was filtered off and the filtrate evaporated to dryness. The residue was suspended in acetone/water (50/50, 20 mL) and stirred at room temperature for 1 h before filtration and removal of volatiles *in vacuo* gave a crystalline beige solid that was used without further purification (641 mg, 78%). ^{1}H NMR (500 MHz; DMSO-d_6): δ (ppm) 10.15 (d, $^4J_{HH}$ = 0.9, 1H, O=C*H*), 9.30 (dd, $^3J_{HH}$ = 8.8, $^4J_{HH}$ = 0.8, 1H, ArH), 8.02 (d, $^3J_{HH}$ = 8.8, 1H, ArH), 7.99 (d, $^3J_{HH}$ = 8.0, 1H, ArH), 7.11 (d, $^3J_{HH}$ = 8.0 Hz, 1H, ArH).^{13}C{^{1}H} NMR (500 MHz; DMSO-d_6): δ (ppm) 193.5 (O=*C*H), 154.9 (*C*–OH), 149.8 (*C*–C=O), 138.1 (C), 137.5 (Ar*C*H), 135.1 (*C*–SO_3H), 128.9 (Ar*C*H), 127.1 (C), 116.9 (Ar*C*H), 110.3 (Ar*C*H).

Synthesis of 2-(4-*N*-substituted-3-thiosemicarbazone)-8-hydroxyquinolines (3–5). 2-Formyl-8-hydroxyquinoline was dissolved in dry, degassed ethanol (10 mL) and treated with 1.1 equiv of a suitable 4-*N*-substituted-3-thiosemicarbazide. A drop of acetic acid was added, and the reaction was subsequently refluxed for 4 h. The light yellow, crystalline precipitate that formed was isolated in good yield (>90%) and purity, washed with ether (3 × 10 mL) and air-dried.

2-(4-*N*-Methyl-3-thiosemicarbazone)-8-hydroxyquinoline (3). 4-*N*-methyl-3-thiosemicarbazide (134 mg, 1.27 mmol) was added to 2-formyl-8-hydroxyquinoline (200 mg, 1.15 mmol) to give a light yellow crystalline solid (303.7 mg, 92%). Elem anal Found (calcd) for $C_{12}H_{12}N_4OS$: C, 55.47 (55.37); H, 4.66 (4.65); N, 21.64 (21.52). ^{1}H NMR (500 MHz; DMSO-d_6): δ (ppm) 11.91 (m, 1H, N–N*H*–C=S), 9.83 (m, 1H, C–O*H*), 8.79 (d, $^3J_{HH}$ = 4.5, 1H, CH_3–N*H*–C=S), 8.41 (d, $^3J_{HH}$ = 8.7, 1H, ArH), 8.30 (d, $^3J_{HH}$ = 8.7, 1H, ArH), 8.26 (s, 1H, N=C*H*), 7.43 (t, $^3J_{HH}$ = 7.8, 1H, ArH), 7.38 (dd, $^3J_{HH}$ = 8.1, $^4J_{HH}$ = 1.3, 1H, ArH), 7.10 (dd, $^3J_{HH}$ = 7.5, $^4J_{HH}$ = 1.4, 1H, ArH), 3.06 (d, $^3J_{HH}$ = 4.6 Hz, 3H, CH_3). ^{13}C{^{1}H} NMR (500 MHz; DMSO-d_6): δ (ppm) 178.0 (*C*=S), 153.8 (*C*–OH), 151.9 (*C*–C=N), 141.8 (N=*C*H), 138.1 (C), 136.1 (Ar*C*H), 128.7 (C), 128.0 (Ar*C*H), 118.3 (Ar*C*H), 117.7 (Ar*C*H), 112.1 (Ar*C*H), 30.9 (CH_3). MS (ES$^+$): *m*/*z* (calcd) 261.0800 (261.0732) {M + H$^+$}. HPLC R_t 9.48 min. Crystals suitable for single-crystal X-ray diffraction were grown from methanol by slow evaporation at room temperature.

2-(4-*N*-Ethyl-3-thiosemicarbazone)-8-hydroxyquinoline (4). 4-*N*-ethyl-3-thiosemicarbazide (151 mg, 1.27 mmol) was added to 2-formyl-8-hydroxyquinoline (200 mg, 1.15 mmol) to give a light yellow crystalline solid (290.1 mg, 92%). Elem anal Found (calcd) for $C_{13}H_{14}N_4OS$: C, 56.99 (56.91); H, 5.16 (5.14); N, 20.52 (20.42). ^{1}H NMR (500 MHz; DMSO-d_6): δ (ppm) 11.85 (s, 1H, N–N*H*–C=S), 9.83 (s, 1H, C–O*H*), 8.84 (t, $^3J_{HH}$ = 5.9, 1H, CH_3–N*H*–C=S), 8.42 (d, $^3J_{HH}$ = 8.7, 1H, ArH), 8.30 (d, $^3J_{HH}$ = 8.7, 1H, ArH), 8.27 (s, 1H, N=C*H*), 7.43 (t, $^3J_{HH}$ = 7.8, 1H, ArH), 7.39 (dd, $^3J_{HH}$ = 8.2, $^4J_{HH}$ = 1.4, 1H, ArH), 7.10 (dd, $^3J_{HH}$ = 7.5, $^4J_{HH}$ = 1.4, 1H, ArH), 3.67–3.61 (m, 2H, CH_2), 1.19 (t, $^3J_{HH}$ = 7.1 Hz, 3H, CH_3). ^{13}C{^{1}H} NMR (500 MHz; DMSO-d_6): δ (ppm) 177.4 (*C*=S), 153.8 (*C*–OH), 152.3 (*C*–C=N), 142.4 (N=*C*H), 138.7 (C), 136.5 (Ar*C*H), 129.2 (C), 128.5 (Ar*C*H), 118.8 (Ar*C*H), 118.2 (Ar*C*H), 112.6 (Ar*C*H), 38.9 (CH_2), 14.9 (CH_3). MS (ES$^+$): *m*/*z* (calcd) 275.10 (275.09) {M + H$^+$}. HPLC R_t 10.71 min.

2-(4-*N*-Phenyl-3-thiosemicarbazone)-8-hydroxyquinoline (5). 4-*N*-Phenyl-3-thiosemicarbazide (212 mg, 1.27 mmol) was added to 2-formyl-8-hydroxyquinoline (200 mg, 1.15 mmol) to give a light yellow crystalline solid (369 mg, 90%). Elem anal Found (calcd) for $C_{17}H_{14}N_4OS$: C, 63.32 (63.33); H, 4.29 (4.38); N, 17.26 (17.38). ^{1}H NMR (500 MHz; DMSO-d_6): δ (ppm) 12.24 (s, 1H, C–N*H*–C=S), 10.37 (s, 1H, N–N*H*–C=S), 9.88 (s, 1H, C–O*H*), 8.60 (d, $^3J_{HH}$ = 8.7, 1H, ArH), 8.38 (s, 1H, N=C*H*), 8.31 (d, $^3J_{HH}$ = 8.7, 1H, ArH), 7.57 (d, $^3J_{HH}$ = 7.5 Hz, 2H, ArH), 7.46–7.39 (m, 4H, ArH), 7.25 (t, $^3J_{HH}$ = 7.4, ArH), 7.12 (dd, $^3J_{HH}$ = 7.5, $^4J_{HH}$ = 1.2, 1H, ArH). ^{13}C{^{1}H} NMR (500 MHz; DMSO-d_6):

δ (ppm) 176.5 (*C*═S), 153.4 (*C*–OH), 151.7 (*C*–C═N), 142.9 (N═*C*H), 130.0 (C), 138.2 (C), 136.1 (Ar*C*H), 128.9 (C), 128.2 (Ar*C*H), 128.1 (Ar*C*H), 126.3 (Ar*C*H), 125.6 (Ar*C*H), 118.8 (Ar*C*H), 117.7 (Ar*C*H), 112.1 (Ar*C*H). MS (ES^+): *m*/*z* (calcd) 323.10 (323.09) {M + H^+}. HPLC R_t 13.27 min.

Synthesis of 2-(4-*N*-substituted-3-thiosemicarbazone)-8-hydroxyquinoline-5-sulfonic acids (12–14). 2-Formyl-8-hydroxyquinoline-5-sulfonic acid was suspended in ethanol (20 mL) and treated with 1.1 equiv of a suitable 4-*N*-substituted-3-thiosemicarbazide. The reaction was stirred at room temperature for 12 h under nitrogen. The yellow, crystalline precipitate that formed was isolated in reasonable yield (>80%) and purity, washed with ether (3 × 10 mL) and air-dried.

2-(4-*N*-Methyl-3-thiosemicarbazone)-8-hydroxyquinoline-5-sulfonic acid (12). 4-*N*-methyl-3-thiosemicarbazide (23 mg, 220 μmol) was added to 2-formyl-8-hydroxyquinoline-5-sulfonic acid (50 mg, 200 μmol) to give a yellow crystalline solid (56 mg, 83%). Elem anal Found (calcd) for $C_{12}H_{12}N_4O_4S_2{\cdot}2H_2O$: C, 38.88 (38.29); H, 4.16 (4.28); N, 14.56 (14.88). ^{1}H NMR (500 MHz; DMSO-d_6): δ (ppm) 12.14 (m, 1H, N–N*H*–C═S), 9.24 (d, $^3J_{HH}$ = 9.1, 1H, ArH), 8.89–8.87 (m, 1H, CH_3–N*H*–C═S), 8.54 (d, $^3J_{HH}$ = 9.1, 1H, ArH), 8.38 (s, 1H, N═C*H*), 7.88 (d, $^3J_{HH}$ = 8.0, 1H, ArH), 7.08 (d, $^3J_{HH}$ = 8.0, 1H, ArH), 3.08 (d, $^3J_{HH}$ = 4.5 Hz, 3H, CH_3). ^{13}C{^{1}H} NMR (500 MHz; DMSO-d_6): δ (ppm) 178.0 (*C*═S), 152.5 (*C*–C═N), 150.7 (N═*C*H), 137.9 (C), 135.2 (Ar*C*H), 126.9 (C), 125.1 (Ar*C*H), 118.1 (Ar*C*H), 110.9 (Ar*C*H), 31.0 (*C*H_3). MS (ES^+): *m*/*z* (calcd) 340.03 (340.03) {M + H^+}. HPLC R_t 6.86 min.

2-(4-*N*-Ethyl-3-thiosemicarbazone)-8-hydroxyquinoline-5-sulfonic acid (13). 4-*N*-ethyl-3-thiosemicarbazide (26 mg, 220 μmol) was added to 2-formyl-8-hydroxyquinoline-5-sulfonic acid (50 mg, 200 μmol) to give a yellow crystalline solid (64 mg, 91%). Elem anal Found (calcd) for $C_{13}H_{14}N_4O_4S_2{\cdot}2H_2O$: C, 39.95 (39.99); H, 4.48 (4.65); N, 13.31 (14.35). ^{1}H NMR (500 MHz; DMSO-d_6): δ (ppm) 12.13 (s, 1H, N–N*H*–C═S), 9.28 (d, $^3J_{HH}$ = 9.1, 1H, ArH), 8.96–8.93 (m, 1H, CH_3–N*H*–C═S), 8.58 (d, $^3J_{HH}$ = 9.1, 1H, ArH), 8.41 (s, 1H, N═C*H*), 7.89 (d, $^3J_{HH}$ = 8.1, 1H, ArH), 7.10 (d, $^3J_{HH}$ = 8.1, 1H, ArH), 3.68–3.63 (m, 2H, CH_2), 1.20 (t, $^3J_{HH}$ = 7.1 Hz, 3H, CH_3). ^{13}C{^{1}H} NMR (500 MHz; DMSO-d_6): δ (ppm) 177.0 (*C*═S), 152.2 (*C*–C═N), 150.5 (N═*C*H), 135.3 (Ar*C*H), 127.0 (C), 125.2 (Ar*C*H), 118.2 (Ar*C*H), 110.8 (Ar*C*H), 38.5 (*C*H_2), 14.4 (*C*H_3). MS (ES^+): *m*/*z* (calcd) 354.04 (354.05) {M + H^+}. HPLC R_t 7.69 min.

2-(4-*N*-Phenyl-3-thiosemicarbazone)-8-hydroxyquinoline-5-sulfonic acid (14). 4-*N*-Phenyl-3-thiosemicarbazide (37 mg, 220 μmol) was added to 2-formyl-8-hydroxyquinoline-5-sulfonic acid (50 mg, 200 μmol) to give an orange crystalline solid (70 mg, 88%). Elem anal Found (calcd) for $C_{17}H_{14}N_4O_4S_2$: C, 50.64 (50.74); H, 3.60 (3.51); N, 13.84 (13.92). ^{1}H NMR (500 MHz; DMSO-d_6): δ (ppm) 12.44 (s, 1H, C–N*H*–C═S), 10.42 (s, 1H, N–N*H*–C═S), 9.24 (d, $^3J_{HH}$ = 9.1, 1H, ArH), 8.70 (d, $^3J_{HH}$ = 9.1, 1H, ArH), 8.48 (s, 1H, N═C*H*), 7.89 (d, $^3J_{HH}$ = 8.1 Hz, 2H, ArH), 7.58–7.56 (m, 2H, ArH), 7.44–7.40 (m, 2H, ArH), 7.28–7.25 (m, 2H, ArH), 7.08 (d, $^3J_{HH}$ = 8.1, 1H, ArH). ^{13}C{^{1}H} NMR (500 MHz; DMSO-d_6): δ (ppm) 176.7 (*C*═S), 152.6 (*C*–C═N), 150.5 (N═*C*H), 138.9 (C), 137.3 (C), 135.2 (Ar*C*H), 128.1 (Ar*C*H), 127.1 (C), 126.4 (Ar*C*H), 125.8 (Ar*C*H), 125.3 (Ar*C*H), 118.5 (Ar*C*H), 110.8 (Ar*C*H). MS (ES^+): *m*/*z* (calcd) 403.05 (403.05) {M + H^+}. HPLC R_t 9.67 min.

Synthesis of 2-(4-*N*-substituted-3-thiosemicarbazonato)-8-quinolinolato copper(II) complexes (6–8). 2-(4-*N*-substituted-3-thiosemicarbazone)-8-hydroxyquinoline was dissolved in DMF (5 mL) and treated with an excess (1.2 equiv) of copper(II)acetate. The reaction darkened considerably whilst stirring at room temperature for 4 h. Addition of water (5–10 mL) precipitated a dark red solid that was collected, washed repeatedly with water (3 × 5 mL) and dried *in vacuo*.

2-(4-*N*-Methyl-3-thiosemicarbazonato)-8-quinolinolato copper(II) (6). 2-(4-*N*-methyl-3-thiosemicarbazone)-8-hydroxyquinoline (50 mg, 192 μmol) reacted with Cu(II)$(OAc)_2{\cdot}2H_2O$ (46 mg, 230 μmol) to give a dark red solid (57.1 mg, 92%). Elem anal Found (calcd) for $C_{12}H_{10}N_4OSCu$: C, 44.94 (44.78); H, 3.03 (3.13); N, 17.39 (17.41). MS (ES^+): *m*/*z* (calcd) 321.9943 (321.9944) {M + H^+}.

2-(4-*N*-Ethyl-3-thiosemicarbazonato)-8-quinolinolato copper(II) (7). 2-(4-*N*-ethyl-3-thiosemicarbazone)-8-hydroxyquinoline (61.8 mg, 225 μmol) reacted with Cu(II)$(OAc)_2{\cdot}2H_2O$ (54 mg, 270 μmol) to give a dark red solid (66.4 mg, 89%). Elem anal Found (calcd) for $C_{13}H_{12}N_4OSCu$: C, 46.55 (46.49); H, 3.70 (3.60); N, 16.68 (16.68). MS (ES^+): *m*/*z* (calcd) 336.0099 (336.0100) {M + H^+}.

2-(4-*N*-Phenyl-3-thiosemicarbazonato)-8-quinolinolato copper(II) (8). 2-(4-*N*-phenyl-3-thiosemicarbazone)-8-hydroxyquinoline (87.8 mg, 272 μmol) reacted with Cu(II)$(OAc)_2{\cdot}2H_2O$ (73 mg, 363 μmol) to give a dark red solid (73.1 mg, 96%). Elem anal Found (calcd) for $C_{17}H_{12}N_4OSCu$: C, 53.20 (53.18); H, 3.28 (3.15); N, 14.47 (14.59). MS (ES^+): *m*/*z* (calcd) 384.0099 (384.0100) {M + H^+}.

Synthesis of 2-(4-*N*-substituted-3-thiosemicarbazonato)-8-quinolinolato-5-sulfonic acid copper(II) complexes (15–17). 2-(4-*N*-substituted-3-thiosemicarbazone)-8-hydroxyquinoline-5-sulfonic acid was dissolved in DMF (2 mL) and treated with an excess (1.2 equiv) of copper(II)acetate. The reaction darkened considerably whilst stirring at room temperature for 4 h. Addition of ether (5–10 mL) precipitated a brown solid that was collected, washed with ether (3 × 5 mL) and air-dried. The crude product was dissolved in a minimal volume of water and passed through a cation-exchange column to remove excess Cu^{2+}. The product was obtained as a dark solid after the removal of water.

2-(4-*N*-Methyl-3-thiosemicarbazonato)-8-quinolinolato-5-sulfonic acid copper(II) (15). 2-(4-*N*-methyl-3-thiosemicarbazone)-8-hydroxyquinoline-5-sulfonic acid (20 mg, 59 μmol) reacted with Cu(II)$(OAc)_2{\cdot}2H_2O$ (14 mg, 70 μmol) to give a dark solid (20.5 mg, 86%). Elem anal Found (calcd) for $C_{12}H_{10}N_4O_4S_2Cu{\cdot}3H_2O$: C, 31.51 (31.61); H, 3.64 (3.54); N, 11.74 (12.29). MS (ES^+): *m*/*z* (calcd) 401.95 (401.94) {M + H^+}.

2-(4-*N*-Ethyl-3-thiosemicarbazonato)-8-quinolinolato-5-sulfonic acid copper(II) (16). 2-(4-*N*-ethyl-3-thiosemicarbazone)-8-hydroxyquinoline-5-sulfonic acid (20 mg, 56 μmol) reacted with Cu(II)$(OAc)_2{\cdot}2H_2O$ (13.5 mg, 68 μmol) to give a dark solid (19.8 mg, 85%). Elem anal Found (calcd) for $C_{13}H_{12}N_4O_4S_2Cu{\cdot}2H_2O$: C, 34.43 (34.55); H, 3.49 (3.57); N, 11.69 (12.40). MS (ES^+): *m*/*z* (calcd) 415.97 (414.96) {M + H^+}.

2-(4-*N*-Phenyl-3-thiosemicarbazonato)-8-quinolinolato-5-sulfonic acid copper(II) (17). 2-(4-*N*-phenyl-3-thiosemicarbazone)-8-hydroxyquinoline-5-sulfonic acid (20 mg, 54 μmol) reacted with $Cu(II)(OAc)_2 \cdot 2H_2O$ (13 mg, 65 μmol) to give a dark solid (22.3 mg, 87%). Elem anal Found (calcd) for $C_{17}H_{12}N_4O_4S_2Cu \cdot 5H_2O$: C, 36.89 (36.85); H, 3.37 (4.00); N, 10.06 (10.11). MS (ES^+): *m/z* (calcd) 463.97 (463.96) $\{M + H^+\}$.

Cell culture conditions and treating with Cu^{II} complexes of hydroxyquinoline-thiosemicarbazone ligands. SH-SY5Y neuron-like cells were grown in DMEM:F-12 media (Invitrogen) supplemented with 10% (v/v) foetal bovine serum, 50 mM Hepes, non-essential amino acids (Invitrogen), and penicillin/streptomycin sulfate (Invitrogen). Cultures were maintained at 37 °C in a humidified incubator with 5% (v/v) CO_2 and passaged every 4–5 days at a dilution of 1/5. Prior to treating with Cu^{II} complexes of hydroxyquinoline-thiosemicarbazone ligands, cells were seeded into 6 well plates at 4×10^4 cells cm^{-2}, and allowed to grow for 2 days. For treating, media was aspirated from the cells then replaced with serum free media containing the treatment compounds at 1, 5 or 10 μM. The compounds were prepared in DMSO at a stock concentration of 1 mM, 5 mM or 10 mM. Stock solutions were diluted 1000-fold in the treatment media (final DMSO content = 0.1% (v/v)), and 0.1% (v/v) DMSO was therefore used as the relevant vehicle control. All treatments were for 1 h at 37 °C in a humidified incubator with 5% (v/v) CO_2. After 1 h, cells were scraped into the existing treatment media then pelleted by centrifugation (1000 × g, 3 min). For Western blot analyses the cell pellets were lysed with Cytobuster Protein Extraction reagent (Novagen) supplemented with EDTA-free protease inhibitor cocktail (Roche), phenylmethanesulfonyl fluoride, sodium fluoride, sodium vanadate, β-glycerophosphate, sodium pyrophosphate, and deoxyribonucleate 5′-oligonucleotido-hydrolase. Cell lysates collected by centrifugation (16,000 × g, 3 min) were normalised for protein content after measuring aliquots using a protein content determination kit (Pierce), then strored at −20 °C. For metal content analysis, the cell pellets were washed twice with phosphate-buffered saline then stored at −20 °C after measuring an aliquot for protein content as above.

Cell toxicity assays. Cell toxicity of treatment compounds was determined after treating cells for 1 h as described above. Two cell toxicity assays were used; the MTS reduction assay (Promega) which measures relative activity of cellular NAD(P)H reductases, and the lactate dehydrogenase (LDH) release assay (Roche) which measures LDH release from cells due to permeabilisation of the plasma membrane. Both assays were performed following manufacturers instructions.

Western blot analysis. Cellular levels of total GSK3β, phoshorylated GSK3β (pGSK3β), total protein kinase B (Akt), pAkt, and β-actin were determined by Western blot analysis of cell lysates described above as previously described.[24] Briefly, proteins were resolved by SDS-PAGE electrophoresis then transferred onto PVDF membranes. Membranes were blocked using skim milk powder then probed for GSK3β, pGSK3, Akt, pAkt, or β-actin using antibodies from Cell Signaling Technology. Membranes were then probed using HRP-linked anti-rabbit secondary antibody, and protein bands detected by enhanced chemiluminescence (GE Healthcare).

Inductively coupled plasma mass spectrometry. Cellular levels of Cu, Fe, and Zn were determined using inductively coupled mass spectrometry as previously described.[24]

Acknowledgements

We thank Assoc. Prof. Kevin Barnham for his pivotal role in initiating this research. We acknowledge funding from the Australian Research Council and National Health Medical Research Council.

Notes and references

1 C. L. Masters, R. Cappai, K. J. Barnham and V. L. Villemagne, *J. Neurochem.*, 2006, **97**, 1700.
2 G. G. Glenner and C. W. Wong, *Biochem. Biophys. Res. Commun.*, 1984, **120**, 885.
3 J. Kang, H. G. Lemaire, A. Unterbeck, J. M. Salbaum, C. L. Masters, K. H. Grzeschik, G. Multhaup, K. Beyreuther and B. Moeller-Hill, *Nature (London, U. K.)*, 1987, **325**, 733.
4 C. L. Masters, G. Simms, N. A. Weinman, G. Multhaup, B. L. McDonald and K. Beyreuther, *Proc. Natl. Acad. Sci. U. S. A.*, 1985, **82**, 4245.
5 J. Marx, *Science (Wash. D. C.)*, 2007, **316**, 1416.
6 H.-C. Huang and Z.-F. Jiang, *J Alzheimers Dis*, 2009, **16**, 15.
7 K. J. Barnham and A. I. Bush, *Curr. Opin. Chem. Biol.*, 2008, **12**, 222.
8 K. J. Barnham, V. B. Kenche, G. D. Ciccotosto, D. P. Smith, D. J. Tew, X. Liu, K. Perez, G. A. Cranston, T. J. Johanssen, I. Volitakis, A. I. Bush, C. L. Masters, A. R. White, J. P. Smith, R. A. Cherny and R. Cappai, *Proc. Natl. Acad. Sci. U. S. A.*, 2008, **105**, 6813.
9 A. I. Bush, *Trends Neurosci.*, 2003, **26**, 207.
10 A. I. Bush, *J. Alzheimer's Dis.*, 2008, **15**, 223.
11 P. S. Donnelly, Z. Xiao and A. G. Wedd, *Curr. Opin. Chem. Biol.*, 2007, **11**, 128.
12 A. R. White, R. Reyes, J. F. B. Mercer, J. Camakaris, H. Zheng, A. I. Bush, G. Multhaup, K. Beyreuther, C. L. Masters and R. Cappai, *Brain Res.*, 1999, **842**, 439.
13 C. J. Maynard, R. Cappai, I. Volitakis, R. A. Cherny, C. L. Masters, Q.-X. Li and A. I. Bush, *J. Inorg. Biochem.*, 2006, **100**, 952.
14 K. J. Barnham, W. J. McKinstry, G. Multhaup, D. Galatis, C. J. Morton, C. C. Curtain, N. A. Williamson, A. R. White, M. G. Hinds, R. S. Norton, K. Beyreuther, C. L. Masters, M. W. Parker and R. Cappai, *J. Biol. Chem.*, 2003, **2778**, 17401.
15 R. A. Himes, G. Y. Park, G. S. Siluvai, N. J. Blackburn and K. D. Karlin, *Angew. Chem. Int. Ed.*, 2008, **47**, 9084.
16 P. A. Adlard, R. A. Cherny, D. I. Finkelstein, E. Gautier, E. Robb, M. Cortes, I. Volitakis, X. Liu, J. P. Smith, K. Perez, K. Laughton, Q. X. Li, S. A. Charman, J. A. Nicolazzo, S. Wilkins, K. Deleva, T. Lynch, G. Kok, C. W. Ritchie, R. E. Tanzi, R. Cappai, C. L. Masters, K. J. Barnham and A. I. Bush, *Neuron*, 2008, **59**, 43.
17 L. Lannfelt, K. Blennow, H. Zetterberg, S. Batsman, D. Ames, J. Harrison, C. L. Maters, S. Targum, A. I. Bush, R. Murdoch, J. Wilson and C. W. Ritchie, *Lancet Neurology*, 2008, **7**, 779.
18 H. Schugar, D. E. Green, M. L. Bowen, L. E. Scott, T. Storr, K. Bohmerle, F. Thomas, D. D. Allen, P. R. Lockman, M. Merkel, K. H. Thompson and C. Orvig, *Angew. Chem. Int. Ed.*, 2007, **46**, 1716.
19 A. R. White, T. Du, K. M. Laughton, I. Volitakis, R. A. Sharples, M. E. Xilinas, D. E. Hoke, R. M. D. Holsinger, G. Evin, R. A. Cherny, A. F. Hill, K. J. Barnham, Q.-X. Li, A. I. Bush and C. L. Masters, *J. Biol. Chem.*, 2006, **281**, 17670.
20 M. Hoshi, M. Sato, S. Matsumoto, A. Noguchi, K. Yasutake, N. Yoshida and K. Sato, *Proc. Natl. Acad. Sci. U. S. A.*, 2003, **100**, 6370.
21 H. Lohi, L. Ianzano, X.-C. Zhao, E. M. Chan, J. Turnbull, S. W. Scherer, C. A. Ackerley and B. A. Minassian, *Hum. Mol. Genet.*, 2005, **14**, 2727.
22 Y. Mao, X. Ge, C. L. Frank, J. M. Madison, A. N. Koehler, M. K. Doud, C. Tassa, E. M. Berry, T. Soda, K. K. Singh, T. Biechele, T. L. Petryshen, R. T. Moon, S. J. Haggarty and L.-H. Tsai, *Cell*, 2009, **136**, 1017.
23 Z. Xiao, P. S. Donnelly, M. Zimmermann and A. G. Wedd, *Inorg. Chem.*, 2008, **47**, 4338.
24 P. J. Crouch, L. W. Hung, P. A. Adlard, M. Cortes, V. Lal, G. Filiz, K. A. Perez, M. Nurjono, A. Caragounis, T. Du, K. Laughton, I. Volitakis,

A. I. Bush, Q.-X. Li, C. L. Masters, R. Cappai, R. A. Cherny, P. S. Donnelly, A. R. White and K. J. Barnham, *Proc. Natl. Acad. Sci. U. S. A.*, 2009, **106**, 381.
25 P. S. Donnelly, A. Caragounis, T. Du, K. M. Laughton, I. Volitakis, R. A. Cherny, R. A. Sharples, A. F. Hill, Q.-X. Li, C. L. Masters, K. J. Barnham and A. R. White, *J. Biol. Chem.*, 2008, **283**, 4568.
26 A. R. Cowley, J. R. Dilworth, P. S. Donnelly and J. M. White, *Inorg. Chem.*, 2006, **45**, 496.
27 H. Zhang, R. Thomas, D. Oupicky and F. Peng, *J. Biol. Inorg. Chem.*, 2008, **13**, 47.
28 P. J. Blower, T. C. Castle, A. R. Cowley, J. R. Dilworth, P. S. Donnelly, E. Labisbal, F. E. Sowrey, S. J. Teat and M. J. Went, *Dalton Trans.*, 2003, 4416.
29 E. Bermejo, A. Cstineiras, L. J. Ackerman, M. D. Owens and D. X. West, *Z. Anorg. Allg. Chem.*, 2001, **627**, 1966.
30 A. R. Cowley, J. R. Dilworth, P. S. Donnelly, A. D. Gee and J. M. Heslop, *Dalton Trans.*, 2004, 2404.
31 F. Basuli, M. Ruf, C. G. Pierpont and S. Bhattacharya, *Inorg. Chem.*, 1998, **37**, 6113.
32 J. L. J. Dearling and P. J. Blower, *Chem. Commun.*, 1998, 2531.
33 R. I. Maurer, P. J. Blower, J. R. Dilworth, C. A. Reynolds, Y. Zheng and G. E. D. Mullen, *J. Med. Chem.*, 2002, **45**, 1420.
34 K. A. Price, A. Caragounis, B. M. Paterson, G. Filiz, I. Volitakis, C. L. Masters, K. J. Barnham, P. S. Donnelly, P. J. Crouch and A. R. White, *J. Med. Chem.*, 2009, **52**, 6606.
35 A. Caragounis, T. Du, G. Filiz, K. M. Laughton, I. Volitakis, R. A. Sharples, R. A. Cherny, C. L. Masters, S. C. Drew, A. F. Hill, Q.-X. Li, P. J. Crouch, K. J. Barnham and A. R. White, *Biochem. J.*, 2007, **407**, 435.
36 T. M. Malm, H. Iivonen, G. Goldsteins, V. Keksa-Goldsteine, T. Ahtoniemi, K. Kanninen, A. Salminen, S. Auriola, T. Van Groen, H. Tanila and J. Koistinaho, *J. Neurosci.*, 2007, **27**, 3712.
37 D. A. E. Cross, D. R. Alessi, P. Cohen, M. Andjelkovich and B. A. Hemmings, *Nature (London, U. K.)*, 1995, **378**, 785.
38 F. Q. Schafer and G. R. Buettner, *Free Radical Biol. Med.*, 2001, **30**, 1191.
39 *CrysAlis CCD*; V.1.171.32.5 Oxford Diffraction Ltd., 2007.
40 *SHELX97 [Includes SHELXS97, SHELXL97] – Programs for Crystal Structure Analysis V. Release 97-2*, Institut fur Anorganische Chemie der Universitat, 1998.
41 L. J. Farrugia, *J. Appl. Crystallogr.*, 1999, **32**, 837.
42 *V.ORTEP-3 v. 1.0.2*Oak Ridge National Laboratory, 1998.
43 M. Hassani, W. Cai, D. C. Holley, J. P. Lineswala, B. R. Maharjan, G. R. Ebrahimian, H. Seradj, M. G. Stocksdale, F. Mohammadi, C. C. Marvin, J. M. Gerdes, H. D. Beall and M. Behforouz, *J. Med. Chem.*, 2005, **48**, 7733.
44 H. Gershon, M. W. McNeil and A. T. Grefig, *J. Org. Chem.*, 1969, **34**, 3268.
45 H. E. Gottlieb, V. Kotlyar and A. Nudelman, *J. Org. Chem.*, 1997, **62**, 7512.